

Influence of Impact Velocity and Steel Armour Hardness on Breakage of Projectile 14.5×114 API/B32

R. Mikulikova^{1*}, R. Ridky², S. Rolc¹ and J. Krestan¹

¹Military Research Institute, Brno, Czech Republic

²SVS FEM, Inc., Brno, Czech Republic

The manuscript was received on 6 November 2017 and was accepted after revision for publication on 25 March 2018.

Abstract:

The goal of this article was focused on the study of projectile breakage after impact on steel armour depending on projectile impact velocity and steel armour hardness. Steel armour samples of hardness HBW500 and HBW600 were impacted by steel core projectile 14.5×114 API/B32 using three different impact velocities. The depth of the projectile penetration into steel armour of hardness HBW400, which was placed 65 mm behind the steel armour samples, was measured. The projectile remains after each impact were searched for their evaluation. For better visualization of the projectile breaking process after the impact on steel armour, the numerical simulations were performed. Experimental and numerical results were compared and combined in a graph showing the dependence of the depth of penetration on the projectile impact velocity for two different steel armour hardnesses and with indication of projectile coherence after impact.

Keywords:

projectile breakage, impact velocity, hardness, depth of penetration

1. Introduction

Necessity to enhance the ballistic protection level of armoured vehicles still increases. One of the higher protection levels is K4 according to STANAG 4569, AEP-55, Volume 1, Edition C. The ballistic protection level K4 is represented by the projectile

* Corresponding author: Military Research Institute, Veslarska 337/230, 637 00 Brno, Czech Republic. E-mail: mikulikova@vubrno.cz

14.5×114 API/B32 with steel core and the standardized impact velocity of 911 ± 20 m/s [1]. The projectile weight is 64 g and the steel core weight is 40 g.

One of the mechanisms of armour developed with the intention to defeat the projectile is to break the projectile core and stop the projectile remains. For research and development of enhanced armour protection, it is very useful to know the projectile breaking conditions. Projectile behaviour after the impact on the armour is influenced by many factors. Two main factors are the armour material hardness and the projectile impact velocity [2, 3].

In some cases of projectile/armour material interactions, a specific phenomenon called “shatter-gap“ occurs. The classical shatter-gap is exhibited when the projectile core is shattered and thereby defeated by the armour when impacted at relatively high velocities. At lower velocities, the projectile could however defeat the armour because the impact energy is insufficient to break the projectile core. This usually results in projectile/armour combinations having multiple ballistic limit values. The classical shatter-gap phenomenon is most common with ceramic armour systems [1].

Nevertheless, armour steel is still the most common armour material, so the goal of this work was the study of projectile breakage after the impact on steel armour depending on the projectile impact velocity and steel armour hardness.

2. Methodology

2.1. Experimental Testing

Steel armour plates were impacted by the projectile 14.5×114 API/B32 with hardened steel core using three different impact velocities: 690 ± 20 m/s, 911 ± 20 m/s and 980 ± 20 m/s. Three following set-ups of steel armour plates of different Brinell hardness (HBW) were tested (plate thickness is behind slash):

- Set-up 1: steel armour plate HBW 400 / 50.7 mm.
- Set-up 2: steel armour plate HBW 500 / 8.3 mm + air gap / 65 mm + steel armour plate HBW 400 / 50.7 mm.
- Set-up 3: steel armour plate HBW 600 / 8.3 mm + air gap / 65 mm + steel armour plate HBW 400 / 50.7 mm.

The scheme of general experimental set-up is shown in Fig. 1. The distance of the target from the muzzle was 18 m.

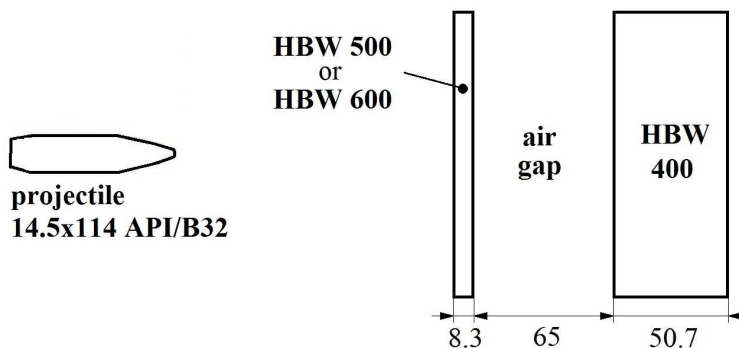


Fig. 1 Experimental set-up

The depth of the projectile penetration into the steel armour of hardness HBW 400 was measured. The projectile remains after each impact were searched for their evaluation. Unfortunately, not all the projectile remains during experimental tests were found.

Some shots were repeated to confirm the results. Repeated shots were not averaged, each shot was included in the table and graph separately.

2.2. Numerical Simulation

The numerical simulations were performed by LS-Dyna software package, the software for non-linear dynamic finite element analysis. The numerical modelling was performed for all the three different steel armour set-ups mentioned in Chapter 2.1. For each velocity range, only one impact velocity was chosen and simulated. At the start of the simulation, the projectile was situated just in front of the first plate of the armour set-up with the defined impact velocity. Simulations for Set-ups 2 and 3 were performed for two yaw angles from projectile flight path, i.e. 0° and 3° . The depth of the projectile penetration into the steel armour of hardness HBW 400 and the projectile residual mass were evaluated.

For the projectile, as well as for the armour steel parts, the Johnson-Cook material model was used, i.e. the empirical constitutive relation used to capture large strains and high strains rates along with the damage evolution and failure of the metal materials [4-7].

3. Results and Discussion

3.1. Set-up 1

Experimental and numerical results for Set-up 1 “steel armour plate HBW 400/50.7 mm” are stated in Tab. 1 and Fig. 2.

Tab. 1 Results for Set-up 1

Projectile impact velocity [m/s]	Experimental testing	Numerical simulation for yaw angle 0°	
	Projectile depth of penetration [mm]	Projectile depth of penetration [mm]	Projectile residual mass [g]
689.5	22.6	19.5	34.8
926.8	28.0	27.6	28.9
988.3	27.5	30.0	27.8

According to the experimental results shown in Tab. 1 and Fig. 2, the depth of the projectile penetration (DOP) increases with the increasing impact velocity from 23 mm for the velocity of 689.5 m/s to 28 mm for the velocity of 926.8 m/s. For the highest projectile impact velocity of 988.3 m/s, the DOP stays similar.

According to the numerical results, the dependence of the DOP on the projectile impact velocity is almost linear. The residual mass of the projectile is almost linear, too, and it corresponds to the DOP dependence which means the higher projectile impact velocity, the higher DOP and the lower projectile residual mass. For the lower velocity, the residual mass is only about 5 g lower than the original weight of projectile core, for the middle and higher velocities, the residual mass is about 11 – 12 g lower than the original weight of the projectile core.

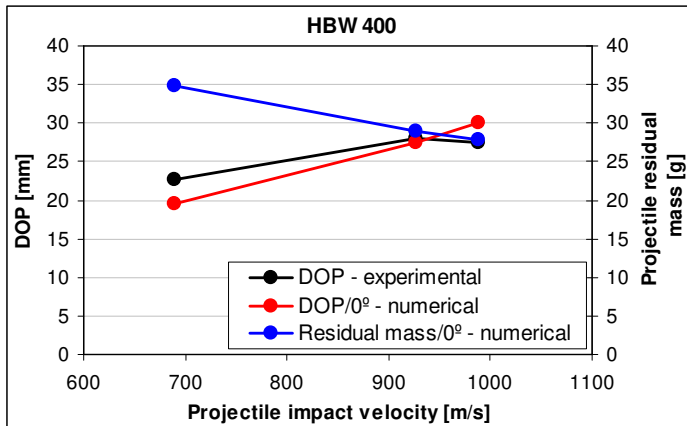


Fig. 2 Dependence of projectile depth of penetration (DOP) and projectile residual mass on projectile impact velocity for Set-up 1

The numerical results of the projectile residual mass were confirmed by the experimental tests. Fig. 3 shows the projectile core remains for the lower and middle impact velocity. At the lower velocity, the projectile core was not broken, at the middle velocity the core was broken probably into two or three parts.



Fig. 3 Remains of projectile 14.5x114 API/B32 found after impact on Set-up 1

Resulting models of the numerical simulation of projectile impact into Set-up 1 are shown in Fig. 4.

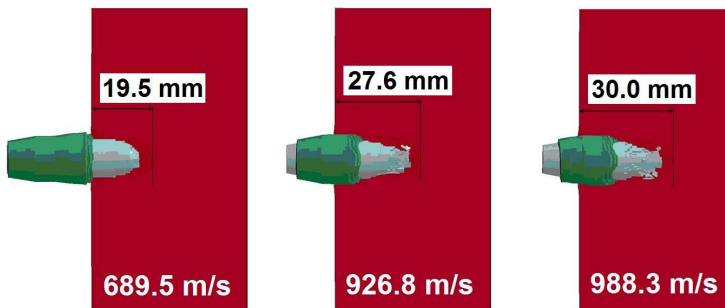


Fig. 4 Numerical simulation for Set-up 1 for yaw angle 0°

Experimental testing and numerical modelling of Set-up 1 was performed with regards to have a reference for the comparison with Set-ups 2 and 3.

3.2. Set-up 2

Both the experimental and numerical results for Set-up 2 “steel armour plate HBW 500/8.3 mm + air gap/65 mm + steel armour plate HBW 400/50.7 mm” are stated in Tab. 2 and Fig. 5.

Tab. 2 Results for Set-up 2

Projectile impact velocity [m/s]	Experimental testing	Numerical simulation for yaw angle 0°		Numerical simulation for yaw angle 3°	
	Projectile depth of penetration [mm]	Projectile depth of penetration [mm]	Projectile residual mass [g]	Projectile depth of penetration [mm]	Projectile residual mass [g]
511.7	10.0	—	—	—	—
673.0	15.5	—	—	—	—
690.1	18.5	7.3	36.8	4.7	29.7
907.8	4.6	—	—	—	—
916.9	2.6	—	—	—	—
930.1	2.6	7.8	6.8	8.4	4.1
983.0	9.0	9.0	14.7	10.3	7.5

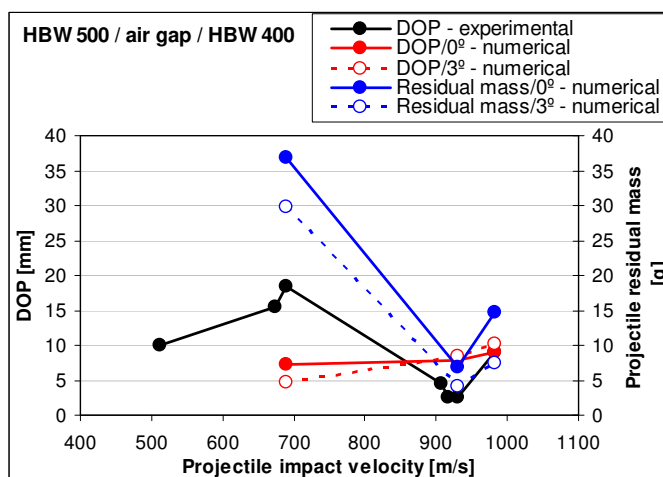


Fig. 5 Dependence of projectile depth of penetration (DOP) and projectile residual mass on projectile impact velocity for Set-up 2

According to the experimental results shown in Tab. 2 and Fig. 5, there is a fall of DOP at the velocity of 911 ± 20 m/s. The DOP fall was confirmed by two other shots at the same velocity range. Because of this non-linear dependence, even the lower impact velocity of around 500 m/s was tested. The whole curve of the experimental DOP indicates the shatter-gap influence. This means that for the velocity of around 690 m/s, the projectile has a higher ballistic efficiency while for the velocity of around 911 m/s, the projectile has a lower ballistic efficiency. The projectile ballistic efficiency at the velocities of around 500 m/s and 980 m/s is similar.

According to the found projectile remains shown in Fig. 6, the projectile starts to break at the impact velocity of around 673 m/s. The projectile breakage could be also influenced by the yaw angle from the impacting projectile flight path. In this case, the projectile at the velocity of 690 m/s was probably not broken due to the yaw angle of about 0° and the projectile at the velocity of 673 m/s could be broken due to the yaw angle greater than 0° .

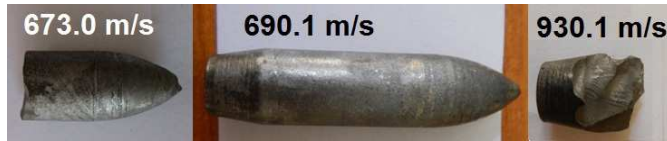


Fig. 6 Remains of projectile 14.5x114 API/B32 found after impact on Set-up 2

The greater yaw angle can be estimated from the shape of the hole in the frontal armour plate caused by projectile perforation. If the yaw angle is about 0° , the hole is round. If the yaw angle is greater than 0° , the ideal round shape of the hole is deformed.

The hole after the perforation of the projectile at the velocity of 690 m/s is almost round (see Fig. 7), which means that the yaw angle was about 0° and the projectile did not break (see Fig. 6); moreover, it resulted in a greater DOP. Vice versa, the hole after the perforation of the projectile at the velocity of 673 m/s is deformed (see Fig. 7), which means that the yaw angle was greater than 0° and the projectile broke (see Fig. 6) and resulted in a lower DOP.

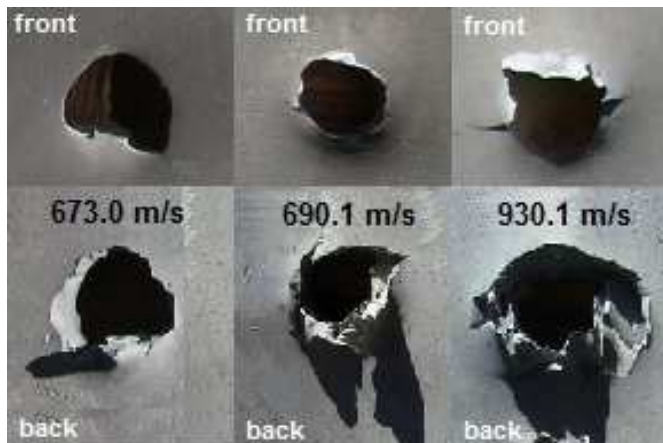


Fig. 7 Perforation of steel armour plate HBW 500/8.3 mm after projectile impact

According to the numerical results, the dependence of the DOP on the projectile impact velocity is almost linear, which does not correspond with the experimental results. On the other hand, the trend of the projectile residual mass curve copies the trend of the experimental DOP curve as well as it corresponds to the size of the found projectile remains (see Fig. 6).

Resulting models of the numerical simulation of the projectile impact into Set-up 2 are shown in Figs. 8 and 9, for yaw angles of 0° and 3° respectively. Numerical modelling confirmed the influence of the yaw angle on the projectile breakage. In case

of the projectile impact velocity of 690 m/s and yaw angle 0° , the projectile did not break (see Fig. 8), however, in case of the projectile impact velocity of 690 m/s and yaw angle 3° , the projectile broke down (see Fig. 9).

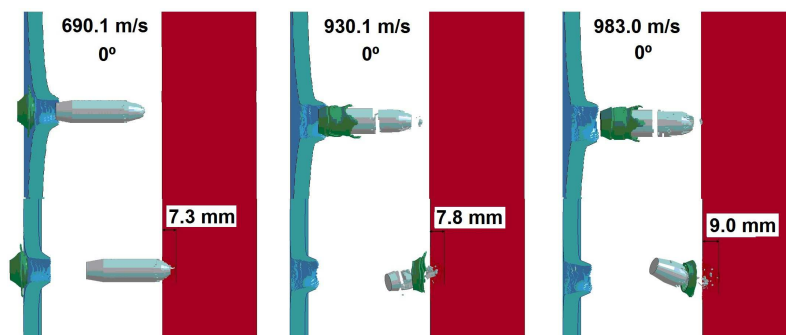


Fig. 8 Numerical simulation for Set-up 2 for yaw angle 0°

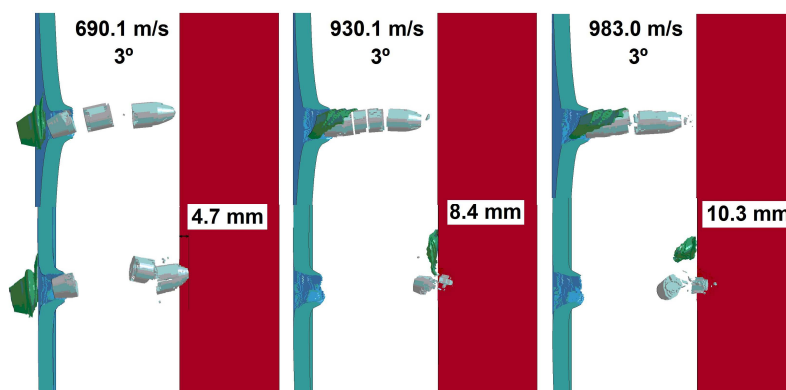


Fig. 9 Numerical simulation for Set-up 2 for yaw angle 3°

3.3. Set-up 3

The experimental and numerical results for Set-up 3 “steel armour plate HBW 600/8.3 mm + air gap/65 mm + steel armour plate HBW 400/50.7 mm” are stated in Tab. 3 and Fig. 10.

Because the goal of this work was to find the projectile impact velocity when the projectile starts to break and because the projectile at the impact velocity of 671.7 m/s broke down, also even the lower impact velocity of around 500 m/s was tested. Fig. 11 shows that the projectile was broken even at such a low velocity.

According to the experimental results shown in Tab. 3 and Fig. 10, the DOP increases very slightly with increasing projectile impact velocity.

Numerical values of the DOP are more or less similar to the experimental ones, especially for the yaw angle 3° . Projectile residual mass decreases quite fast and almost linearly with increasing projectile impact velocity.

Tab. 3 Results for Set-up 3

Projectile impact velocity [m/s]	Experimental testing	Numerical simulation for yaw angle 0°		Numerical simulation for yaw angle 3°	
	Projectile depth of penetration [mm]	Projectile depth of penetration [mm]	Projectile residual mass [g]	Projectile depth of penetration [mm]	Projectile residual mass [g]
503.3	1.3	—	—	—	—
671.7	2.5	—	—	—	—
688.5	0.9	—	—	—	—
689.6	1.5	7.1	35.4	3.2	23.4
910.1	1.9	—	—	—	—
926.0	3.0	4.1	10.8	5.4	4.4
982.5	5.0	7.4	8.4	6.2	3.2

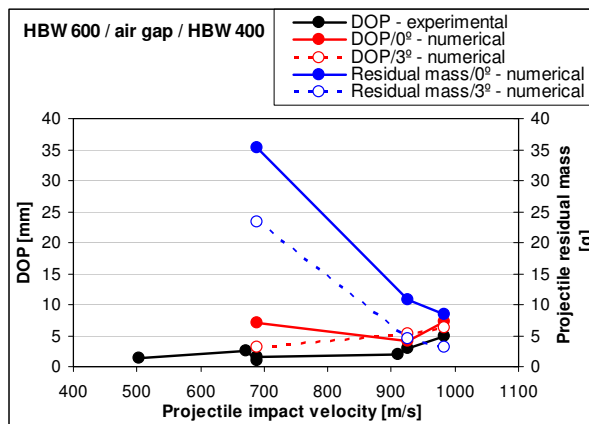


Fig. 10 Dependence of projectile depth of penetration (DOP) and projectile residual mass on projectile impact velocity for Set-up 3

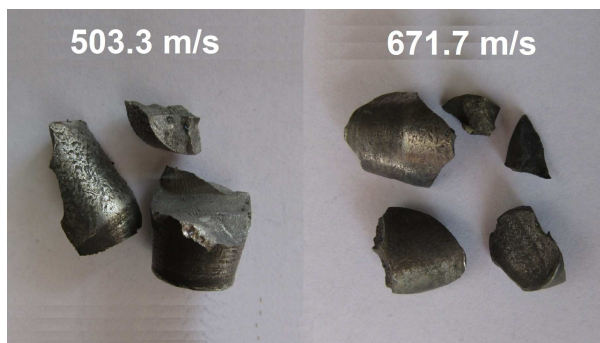


Fig. 11 Remains of projectile 14.5 × 114 API/B32 found after impact on Set-up 3

The resulting models of the numerical simulation of projectile impact into Set-up 3 are shown in Figs. 12 and 13, for the yaw angles of 0° and 3° respectively. Fig. 12 shows the difference from the experimental results with regard to projectile breakage. According to the numerical simulation, the projectile with the impact velocity of 689.6 m/s and the yaw angle 0° does not break. Within the experimental testing, the projectile was broken at the impact velocity of 671.7 m/s and also 503.3 m/s (see Fig. 11).

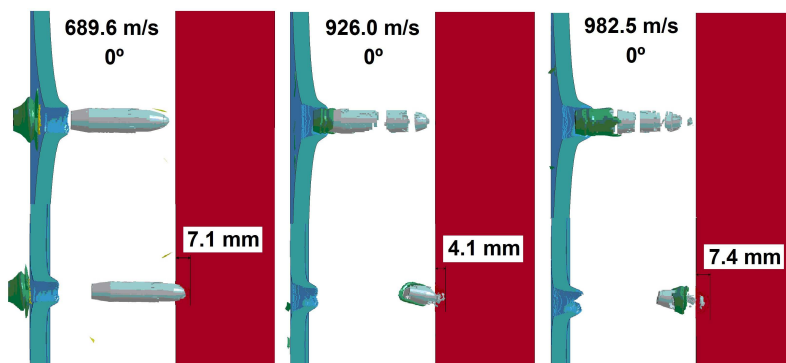


Fig. 12 Numerical simulation for Set-up 3 for yaw angle 0°

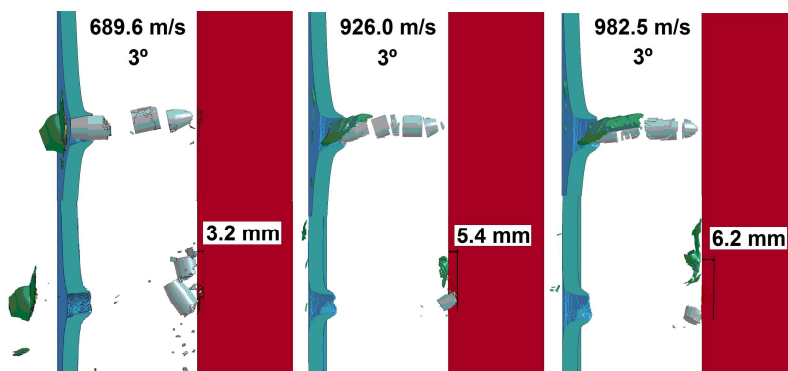


Fig. 13 Numerical simulation for Set-up 3 for yaw angle 3°

4. Conclusion

Three set-ups of steel armour plates of different Brinell hardness (HBW 400, HBW 500 and HBW 600) were ballistically tested by steel core projectile 14.5×114 API/B32 using three different impact velocities: 690 ± 20 m/s, 911 ± 20 m/s and 980 ± 20 m/s. The depth of projectile penetration (DOP) into steel armour of hardness HBW 400 was measured. The projectile remains after each impact were searched for their evaluation. The experimental results were supplemented, combined and compared with the numerical simulations.

For Set-up 1 “steel armour plate HBW 400/50.7 mm“, it was found out that the DOP values correspond to numerical values. The dependences of the DOP and the

residual projectile mass are more or less linear. The higher the impact velocity, the greater the DOP and the smaller the projectile residual mass. The projectile starts to break down at the impact velocity in the range of 911 ± 20 m/s.

For Set-up 2 “steel armour plate HBW 500/8.3 mm + air gap/65 mm + steel armour plate HBW 400/50.7 mm“, it was found out that the DOP values do not correspond to the numerical values. The experimental DOP curve indicates the shatter-gap influence. It means that for the velocity in the range of 690 ± 20 m/s, the projectile has a higher ballistic efficiency, while for the velocity in the range of 911 ± 20 m/s, the projectile has a lower ballistic efficiency. The projectile ballistic efficiency at the velocities of around 500 m/s and 980 m/s is similar. The projectile starts to break at the impact velocity of around 673 m/s, if the yaw angle is greater than 0° . The trend of the numerical projectile residual mass curve copies the trend of the experimental DOP curve, which means that the projectile residual mass, as well as the DOP, are the lowest at the velocity range of 911 ± 20 m/s. According to the combination of both experimental and numerical results, it could be stated that the ballistic efficiency of steel armour plate of hardness HBW 500 and thickness 8.3 mm is the highest at 911 ± 20 m/s and the lowest at 690 ± 20 m/s.

For Set-up 3 “steel armour plate HBW 600/8.3 mm + air gap/65 mm + steel armour plate HBW 400/50.7 mm“, it was found out that the numerical values of the DOP are more or less similar to the experimental ones, especially for the yaw angle of 3° . The DOP increases very slightly with the increasing projectile impact velocity. The projectile residual mass decreases quite fast and almost linearly with increasing projectile impact velocity. Within the experimental testing, the projectile was broken at the impact velocity of 671.7 m/s and also of 503.3 m/s.

Acknowledgement

The work was supported by the Ministry of Defence of the Czech Republic in connection with project OFVVU20150004.

References

- [1] NATO STANDARD AEP-55. *Procedures for Evaluating the Protection Level of Armoured Vehicles – Kinetic Energy and Artillery Threat*. Vol. 1, ed. C, Brussels: NSA, 2014.
- [2] BUCHAR, J., VOLDŘICH, J. *Terminal Ballistics* (in Czech). Prague: Academia, 2003, 340 p. ISBN 80-200-1222-2.
- [3] RYAN, S., LI, H., EDGERTON, M., GALLARDY, D. and CIMPOERU, S.J. The Ballistic Performance of an Ultra-High Hardness Armour Steel: An Experimental Investigation. *International Journal of Impact Engineering*, 2016, vol. 94, p. 60-73. DOI 10.1016/j.ijimpeng.2016.03.011.
- [4] *LS-DYNA Keywords User's Manual*. Materials models, vol. II, revision 3372, 2013.
- [5] JOHNSON G.R. and COOK, W.H. A Constitutive Model and Data for Metals Subjected to Large Strains, High Strain Rates and High Temperatures. In: *Proceeding of the Seventh International Ballistics Symposium*, The Hague, p. 541-547.

- [6] JOHNSON G.R. and COOK, W.H. Fracture Characteristics of Three Metals Subjected to Various Strain, Strain Rates, Temperatures and Pressures. *Engineering Fracture Mechanics*, 1985, vol. 21, no. 1, p. 31-48.
- [7] RIDKY, R. et al. Simulation as a Reliable Tool for Predicting the Degree of Armor Damage. In: *International Conference on Military Technologies*. Brno: University of Defence, 2015, p. 717-723. DOI 10.1109/MILTECHS.2015.7153742.